POLSKA AKADEMIA NAUK
INSTYTUT MASZYN PRZEPŁYWOWYCH

PRACE INSTYTUTU MASZYN PRZEPŁYWOWYCH

TRANSACTIONS
OF THE INSTITUTE OF FLUID-FLOW MACHINERY

69

WARSZAWA–POZNAŃ 1975
PAŃSTWOWE WYDAWNICTWO NAUKOWE

PRACE INSTYTUTU MASZYN PRZEPŁYWOWYCH

poświęcone są publikacjom naukowym z zakresu teorii i badań doświadczalnych w dziedzinie mechaniki i termodynamiki przepływów, ze szczególnym uwzględnieniem problematyki maszyn przepływowych

*

THE TRANSACTIONS OF THE INSTITUTE OF FLUID-FLOW MACHINERY

exist for the publication of theoretical and experimental investigations of all aspects of the mechanics and thermodynamics of fluid-flow with special reference to fluid-flow machinery

REDAKCJA EDITORIAL OFFICE
Instytut Maszyn Przepływowych PAN,
80-952 Gdańsk, skr. pocztowa 621, ul. Gen. Józefa Fiszera 14, tel. 41-12-71

Printed in Poland

PAŃSTWOWE WYDAWNICTWO NAUKOWE – ODDZIAŁ W POZNANIU

Nakład 380+90 egz.	Oddano do składania 7 III 1975 r.
Ark. wyd. 14,75 Ark. druk. 11,5	Podpisano do druku 2 XII 1975 r.
Papier druk sat. kl. V, 62 g 70×100 cm.	Druk ukończono w grudniu 1975 r.
Nr zam. 259/91.	R-15/876. Cena zł 45,–

DRUKARNIA UNIWERSYTETU IM. A. MICKIEWICZA W POZNANIU

PRACE INSTYTUTU MASZYN PRZEPŁYWOWYCH
1975 Zeszyt 69

JERZY KRZYŻANOWSKI

Gdańsk

On the Erosion Rate — Droplet Size Relation*

There is still little known about the droplet size-erosion rate patterns for wet steam turbine stages. It has been already proved that the structure of the droplet stream may influence very much some of the impact parameters governing the erosion of the turbine blading [1]. In order to shed more light on the problem, a series of experiments was initiated at Institute of Fluid-Flow Machinery. In the test stand of I. F. F. M. the structure of the droplet stream may be readily controlled. The aim of this report is to present the algorithm relating the structure of the droplet stream in the mentioned stand with some impact parameters. Also an attempt is made toward preliminary evaluation of the experimental results presented in [3].

Nomenclature

$A' = \sqrt{\dfrac{0{,}85\mu\rho}{r_*^3 \rho_*^2 c_1}}$,

c_1 — air velocity [m/s],

c_* — droplet velocity [m/s],

D — mean diameter of the rotor [m],

D_s — mean diameter of the sample [m],

E_r — rationalized erosion rate,

F — see Fig. 3 [m],

$F(\varphi)$ — see eq. (14),

G — constant [m³/s²],

$f_n \equiv \dfrac{1}{\Delta r_*} \dfrac{n(r_*, c_1)}{N}$ — number distribution function [l/m],

k — factor of proportionality, see Fig. 4 [mg/m],

L — see Fig. 3 [m],

L_s — sample length [m],

$n(r_*, c_1)$ — number of the droplets of a given size r_* per unit area and the droplet stream layer thickness ΔR_1 [1/m²],

N — number of all droplets per unit area and per the droplet stream layer thickness ΔR_1 [1/m²],

N_a — normalized erosion resistance,

$N_{1,2,3}$ — constants,

r_* — droplet radius [m],

u — circumferential velocity [m/s],

U_a — water flux over the sample surface [m³/m²s],

UA — see (18),

$\bar{U}_a$ — mean value of U_a [m³/m²s],

$\overline{UA}$ — see (19),

U_{eM} — meximum instantaneous value of the volumetric material loss per unit area and unit time [m³/m²s],

UEM — see (23),

$\bar{U}_{eM}$ — mean value of U_{eM} [m³/ms],

$\overline{UEM}$ — see (24),

w_* — droplets velocity in the relative frame of reference [m/s],

w_{*N} — normal component of w_* [m/s],

$\underset{M}{\bar{w}}_{*N}$, $\underset{M}{\bar{\bar{w}}}_{*N}$ — mean values of w_{*N} [m/s],

w_1 — air velocity in the relative frame of reference [m/s],

α, γ — see Fig. 2 [dgr],

* Praca wykonana w ramach problemu resortowego PAN-19, grupa tematyczna 2.

Δm – loss of material eroded [mg],
ΔM_* – amount of water supplied onto the trailing edge of the flat plate per its length ΔR_1 [kg/s],
ΔR_1 – the length element of the trailing edge of the flat plate [m],
$\Delta(\Delta m)/\Delta\tau$ – the maximum slope of the curve $\Delta m = f(\tau)$ [mg/min],
μ – viscosity of air [kg/ms],
φ, φ_n – see Fig. 3 [dgr],
ρ – density of air [kg/m^3],
ρ_* – density of water [kg/m^3],
τ – time [min].

1. Introduction

There are some characteristic features of the kinematics of a droplet motion in the axial gap of a steam turbine blading.

The neighbourhood of the leading edge of the rotor blade is exposed to the impact of water droplets generated on the trailing edge of the stator blade. The radii of the droplets impacting the blade surface element considered depend upon its distance from the blade leading edge. The further away from the leading edge of the blade the surface element is located, the smaller are the maximum and mean value of the droplet radius. Also the angle of incidence, which is a function of the inclination of the blade surface element and the droplet size, changes.

Another characteristic feature of the droplet impact intensity is its strong dependence upon the structure of the droplet stream. This had been proved in ref. [1], where the correlation between droplet stream structure and the impact parameters was considered.

In the routine experimental investigation of the material removal-time patterns for different materials, these characteristic features of the droplet stream are usually not taken into account. Usually:

1. The droplets, no matter what their size, collide with the sample of the material under the same angle of incidence. Mostly this angle equals to 90°.

2. The structure of the droplet stream is usually relatively homogeneous. In general, little is known about this structure and often not even the droplet stream is used in tests, but rather a liquid jet.

It appears, however, that both the angle of incidence and the droplet structure have substantial influence upon erosion rate patterns. As far as the influence of the angle of incidence is concerned, some information is already available. One comes roughly to the conclusion that the normal component of the impact velocity governs the erosion*. Much less is known about the influence of the droplet size. Only recently (ref. [2]) an attempt was made to draw some preliminary conclusions from the meager experimental data; it is there assumed that the drop size effect can be represented by a factor of the form

$$w_{*N}^2 r_* = \text{const},$$

where the constant represents a critical or threshold combination of normal component of the droplet velocity and droplet radius, such that, for $w_{*N}^2 r \leqslant$ constant no significant erosion occurs.

* See extensive reference data in ref. [2].

In order to shed more light on the droplet size effect, among others, a test rig with rotating sample was built in the Institute of Fluid-Flow Machinery of the Polish Academy of Sciences. The sample intersects once per rotation the droplet stream generated in the aerodynamic wake of a flat plate. The particular feature of the stand is that the droplet stream structure may readily be controlled by changing the air velocity in the test section, the amount of water per unit time and unit width of the plate, the length of the plate, the shape of the trailing edge of the plate, etc. Mr. B. Weigle designed the stand; he and Mr. H. Severin were in charge of the experiments. The outline of the stand is shown in Fig. 1. More details are available elsewhere [3].

The aim of this report is to present an algorithm relating the structure of the droplet stream with mean values of some selected impact parameters. Also a preliminary evaluation of the experimental results presented in ref. [3] is made. Among the selected impact parameters particular attention is paid to the mean value of $\bar{w}_{*N}$ of the impact velocity w_{*N}, the mean value $\bar{U}_a$ of the amount of water impinging upon the unit area of the sample per unit time and the mean value $\bar{U}_{eM}$ of the product of U_a and $(w_{*N}/2550)^5$. As explained below it is the ref. [4] which indicates the importance of $\bar{U}_{eM}$ as far as the maximum instantaneous erosion rate is concerned. The structure of the droplet stream is defined by the droplet size distribution function. This function is assumed to be known from the experiments in ref. [3] as a function of droplet radius and air velocity.

2. Formulation

Before we formulate the conditions of the droplet impact with the rotating sample of the I.F.F.M.* experimental stand, let us consider the kinematics of the individual droplet.

In some prior author's papers (see f.ex. ref. [5]), it has been indicated that the droplet motion in the aerodynamic wake may be described with sufficient accuracy by the equation:

$$\frac{c_*}{c_1} = 0{,}8\left\{1 - \frac{1}{[1 + A'z + \sqrt{A'^2 z^2 + 2A'z}]^2}\right\}, \tag{1}$$

c_* is the droplet velocity in the absolute reference frame of coordinates, c_1 – the gas velocity outside of the aerodynamic wake and z – the coordinate as indicated in Fig. 1. A' is a constant relevant to the droplet size and flow conditions. The relationship between the droplet velocity, the gas velocity and droplet size is shown in Fig. 2. The curves given are calculated for:

$$\mu = 1.85 \cdot 10^{-5}\ \text{kg/s}, \quad \rho = 1.205\ \text{kg/m}^3, \quad \rho_* = 1000\ \text{kg/m}^3, \quad z = 0{,}3\ \text{m}.$$

This group of parameters is relevant to the I.F.F.M. stand. The kinematics of the droplets, particularly the droplet path in the absolute and relative reference frames as well

* I. F. F. M. – Institute of Fluid-Flow Machinery of the Polish Academy of Sciences in Gdańsk.

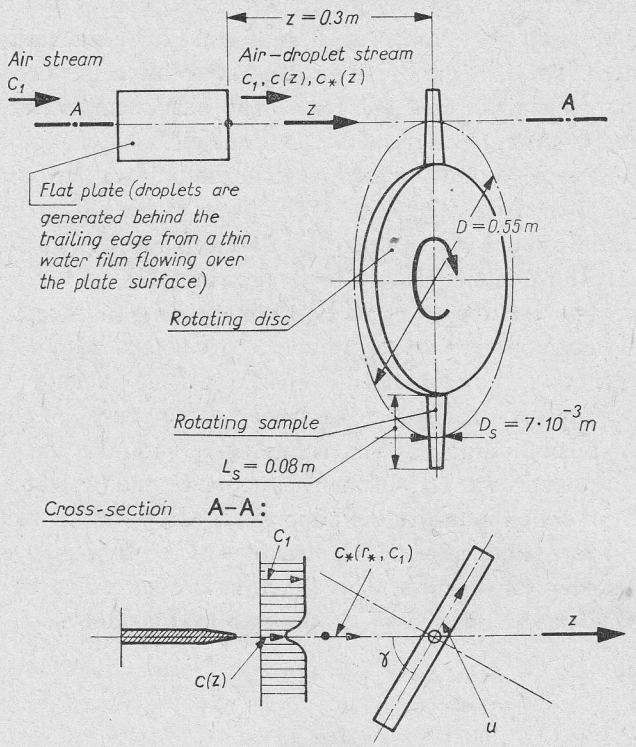

Fig. 1. Scheme of the experimental stand of I.F.F.M. with the rotating sample

as the droplet velocity w_* in the relative reference frame

$$\vec{w}_* = \vec{c}_* - \vec{u} \tag{2}$$

is shown in Fig. 3.

The experiments in ref. [3] have been carried out for 4 air velocities:

$$c_1 = 60, 75, 92 \quad \text{and} \quad 153 \text{ m/s}.$$

Some parameters of droplet kinematics related to the data mentioned above are listed below:

$$U = 200 \text{ m/s}, \quad \gamma = 80°, \quad D_s = 7 \cdot 10^{-3} \text{ m}$$

c_1 [m/s]	60		75		92		153	
r_* [μ]	10	400	10	400	10	400	10	400
w_1 [m/s]	198.5		199.0		200.5		220.0	
w_* [m/s]	197.5	197.5	198.5	197.5	200.5	197.0	214.5	197.0
α [θ]	+3°42′	−5°14′	+7°06′	−4°39′	+10°55′	−3°38′	+23°32′	−0°30′
$\Delta\alpha$ [θ]	3°57′	13°53′	2°00′	13°45′	6°45′	20°18′	7°48′	31°50′

Now the conditions of the droplet impact may be easily calculated under the assumption that the droplet path shown in Fig. 3 does not change its shape in the neighbourhood of the sample. This assumption has been evaluated in ref. [6] in more detail.

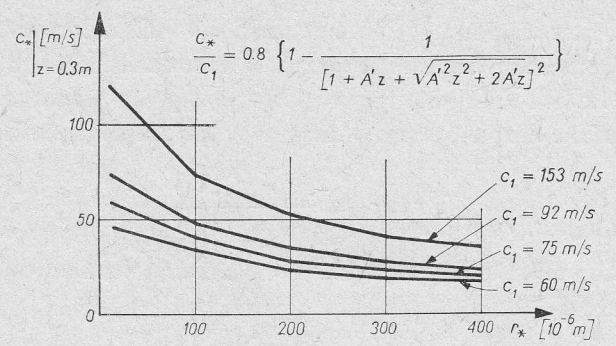

Fig. 2. Some information about the kinematics of the droplet in the IFFM experimental stand

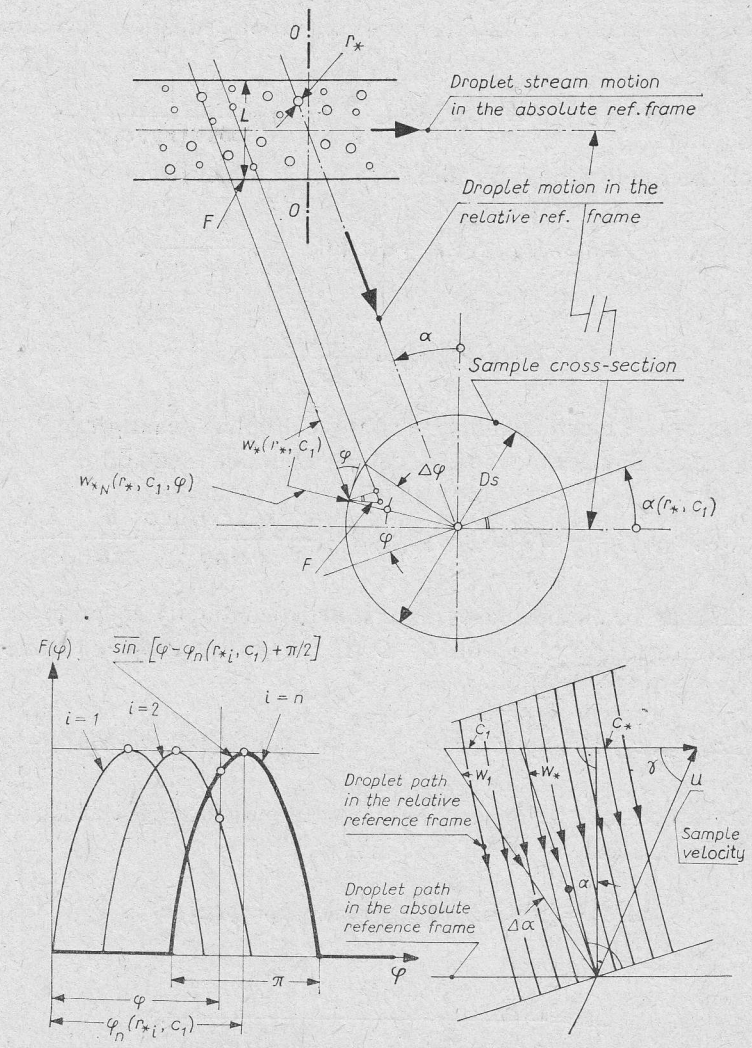

Fig. 3. Kinematics of the individual droplet impact

Let us consider first the amount of water which hits the unit area of the sample per unit time. This parameter of the droplet impact is worth considering because it has been already shown for ex. in ref. [4] that the erosion rate is proportional to it. Let us assume that the structure of the droplet stream is defined by the droplet size distribution function

$$f_n(r_*, c_1) \equiv \frac{1}{\Delta r_*} \frac{n(r_*, c_1)}{N} \tag{3}$$

and that this function in the point where the sample intersects the droplet stream is given by the equation

$$f_n(r_*, c_1) = N_1 r_*^{N_2} e^{-N_3 r_*}. \tag{4}$$

The numbers N_1, N_2, N_3 are experimentally established constants depending on c_1 only.

Then the number of droplets of a particular size r_* impinging upon the surface element $\Delta R_1 \cdot (D_s/2) \cdot d\varphi$ of the sample per one crossing of the droplet stream is, according to Fig. 3, equal to

$$n(r_*, c_1) LF = n(r_*, c_1) L \frac{D_s}{2} d\varphi \sin\varphi \frac{1}{\cos\alpha(r_*, c_1)}. \tag{5}$$

The volume of the water carried by these droplets is equal to

$$\frac{4}{3}\pi r_*^3 \cdot n(r_*, c_1) \cdot L \frac{D_s}{2} d\varphi \sin\varphi \frac{1}{\cos\alpha(r_*, c_1)}. \tag{6}$$

Since

$$\cos\alpha(r_*, c_1) = \frac{u \sin\gamma}{w_*(r_*, c_1)} \tag{7}$$

and the frequency with which the sample crosses the droplet stream per unit time is $u/\pi D$, hence, the volumetric flux relevant to this volume of water is equal to

$$\delta U_a(r_*, c_1, \varphi) = \frac{4}{3}\pi r_*^3 LN f_n(r_*, c_1) \Delta r_* \frac{w_*(r_*, c_1) \sin\varphi}{u \sin\gamma} \cdot \frac{u}{\pi D} \cdot \frac{1}{\Delta R_1}. \tag{8}$$

The product LN may be eliminated by means of the continuity equation for the liquid phase formulated for the cross-section $O-O$ (Fig. 3) of the droplet stream. It has the form:

$$\Delta M_* = \sum_{r_*=0}^{\infty} Lc_*(r_*, c_1) n(r_*) \frac{4}{3}\pi r_*^3 \rho_* = \sum_{r_*=0}^{\infty} Lc_*(r_*, c_1) f_n(r_*, c_1) N \Delta r_* \frac{4}{3}\pi r_*^3 \rho_*. \tag{9}$$

The summation, which may be replaced by integration, is extended over all the droplet radii in the stream. Instead of eq. (9), one may write:

$$\Delta M_* = \tfrac{4}{3}\pi\rho_* LN \int_0^{\infty} r_*^3 f_n(r_*, c_1) c_*(r_*, c_1) dr_*. \tag{10}$$

Hence

$$LN = \frac{\Delta M_*}{\tfrac{4}{3}\pi\rho_* \int_0^{\infty} r_*^3 f_n(r_*, c_1) c_*(r_*, c_1) dr_*}. \tag{11}$$

For the particular droplet size the angle $\alpha(r_*, c_1)$ may be expressed by the equation:

$$\alpha = \operatorname{arc\,tg}(\operatorname{tg}\alpha), \tag{12}$$

where

$$\tan\alpha = \operatorname{sign}\left[\sin\left(\frac{c_*(r_*, c_1) - u\cos\gamma}{w_*(r_*, c_1)}\right)\right]\frac{w_*(r_*, c_1)}{u\sin\gamma}\sqrt{1-\frac{u^2\sin^2\gamma}{w_*^2(r_*, c_1)}}. \tag{13}$$

The sign–function takes care of the appropriate sign of term $\tan\alpha$. The second part of the R-H-S of the eq. (13) may be easily deduced from the geometric relationship shown in Fig. 3. It must be remembered that for each droplet size r_* we obtain a different α or, in other words, $\alpha = \alpha(r_*, c_1)$. Hence, in order to validate the eq. (8) for all droplet sizes, the sin φ function in it must be replaced by function $F(\varphi)$, such that (see Fig. 3):

$$\begin{aligned}
&F(\varphi) = 0 && \text{for} \quad \varphi < \varphi_n(r_*, c_1) - \frac{\pi}{2},\\
&F(\varphi) = \overline{\sin}\left[\varphi - \varphi_n(r_*, c_1) + \frac{\pi}{2}\right] && \text{for} \quad \varphi_n(r_*, c_1) - \frac{\pi}{2} \leqslant \varphi \leqslant \varphi_n(r_*, c_1) + \frac{\pi}{2},\\
&F(\varphi) = 0 && \text{for} \quad \varphi > \varphi_n(r_*, c_1) + \frac{\pi}{2},
\end{aligned} \tag{14}$$

where

$$\varphi_n(r_{*i}, c_1) = \varphi_n(r_{*i-1}, c_1) + \alpha(r_{*i-1}, c_1) - \alpha(r_{*i}, c_1) \tag{15}$$

$$i = 1, 2, 3 \ldots,$$

also,

$$\varphi_n(r_{*0}, c_1) = \frac{\pi}{2} \quad \text{and} \quad \alpha(r_{*0}, c_1) = \alpha(r_{*1}, c_1). \tag{16}$$

Rearranging (8) by means of (11) and (14) results in

$$\delta U_a(r_*, c_1, \varphi) = \frac{1}{\rho_*}\cdot\frac{\Delta M_*}{\Delta R_1}\frac{r_*^3 f_n(r_*, c_1)}{\int_0^\infty r_*^3 f_n(r_*, c_1)\, c_*(r_*, c_1)\, dr_*}\cdot\frac{w_*(r_*, c_1)}{\pi D\,\sin\gamma}\times$$

$$\times\,\overline{\sin}\left[\varphi - \varphi_n(r_*, c_1) + \frac{\pi}{2}\right]\Delta r_*. \tag{17}$$

One establishes the volumetric water flux $U_a(c_1, \varphi)$ for a surface element located by φ extending the integration of the value $\delta U_a(r_*, c_*, \varphi)$ over the whole range of droplet size. Hence one finally obtains:

$$U_a(c_1, \varphi) = \frac{1}{\rho_*}\frac{\Delta M}{\Delta R_1}\frac{1}{\pi D\,\sin\gamma}\int_0^\infty \frac{r^3 f_n(r_*, c_1)\, w_*(r_*, c_1)}{\int_0^\infty r_*^3 f_n(r_*, c_1)\, c_*(r_*, c_1)\, dr_*}\times$$

$$\times\,\overline{\sin}\left[\varphi - \varphi_n(r_*, c_1) + \frac{\pi}{2}\right]dr_* = \frac{1}{\rho_*}\frac{\Delta M_*}{\Delta R_1}\frac{1}{\pi D\,\sin\gamma}UA(c_1, \varphi). \tag{18}$$

In order to eliminate the dependence of φ one may average $U_a(c_1, \varphi)$ over the circumference of the sample. Hence:

$$\bar{U}_a(c_1) = \frac{1}{\varphi_n(r_{*\max}, c_1) + \frac{\pi}{2}} \frac{\frac{1}{\rho_*} \frac{\Delta M_*}{\Delta R_1} \frac{1}{\pi D \sin\gamma}}{\int_0^{\infty} r_*^3 f_n(r_*, c_1) c_*(r_*, c_1) dr_*} \cdot \int_0^{\varphi_n(r_{*\max}, c_1)+\frac{\pi}{2}} \times$$

$$\times \int_0^{\infty} r_*^3 f_n(r_*, c_1) w_*(r_*, c_1) \overline{\sin}\left[\varphi - \varphi_n(r_*, c_1) + \frac{\pi}{2}\right] dr_* d\varphi =$$

$$= \frac{1}{\rho_*} \frac{\Delta M_*}{\Delta R_1} \frac{1}{\pi D \sin\gamma} \overline{UA}(c_1). \tag{19}$$

The erosion rate is obviously not only the function of the flux of water impinging upon the surface element of the rotating sample. It is also a function of the impact velocity. This relationship may be expressed as an empirical equation in the form (ref. [4]):

$$\frac{\Delta m}{\tau} = k \frac{U_a}{N_a} \left(\frac{w_{*N}}{2550}\right)^5 \exp(-0{,}25 \Delta m / \Delta m_T). \tag{20}$$

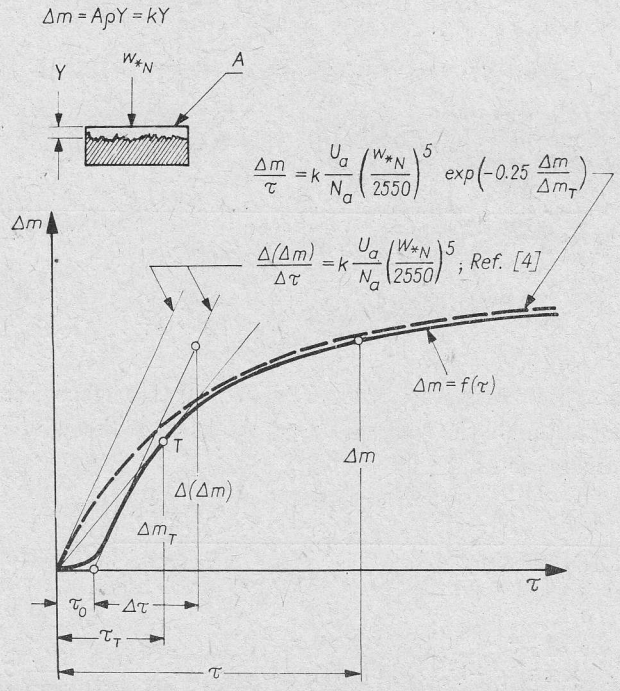

Fig. 4. Characteristic material removal-time pattern, nomenclature, see also (ref. [4])

For a flat sample the coefficient $k = A \cdot \rho$. Other symbols of eq. (20) are explained in Fig. 4. The maximum instantaneous erosion rate $\Delta(\Delta m)/\Delta\tau$ is according to ref. [4] and eq. (20) equal to:

$$\frac{\Delta(\Delta m)}{\Delta\tau} = k \frac{U_a}{N_a} \left(\frac{w_{*N}}{2550} \right)^5 \equiv U_{eM} k \,. \tag{21}$$

These empirical relationships have been established for the flat material sample attacked by a relatively homogeneous (in size and direction) droplet stream. Application of these formulae for the case of cylindrical, rotating samples demands assuming that the erosion damage caused by the droplet groups of a particular size may be superimposed. That assumption has not yet been proved and may be accepted here merely as a first approximation. Under this assumption, the theoretical evaluation of the maximum instantaneous value of erosion rate may be based on the value:

$$\delta U_{eM}(r_*, c_1, \varphi) = \frac{1}{N_a} \delta U_a(r_*, c_1, \varphi) \cdot \left(\frac{w_{*N}(r_*, c_1, \varphi)}{2550} \right)^5 \tag{22}$$

its integral extended over all droplet size:

$$U_{eM}(c_1, \varphi) = \int_0^\infty \delta U_{eM}\, dr_* = \frac{1}{\rho_* N_a} \frac{\Delta M_*}{\Delta R_1} \frac{1}{\pi D \sin\gamma} \int_0^\infty \frac{r_*^3 f_n(r_*, c_1)\, w_*(r_*, c_1)}{\int_0^\infty r_*^3 f_n(r_*, c_1)\, c_*(r_*, c_1)\, dr} \times$$

$$\times \left[\frac{w_{*N}(r_*, c_1, \varphi)}{2550} \right]^5 \overline{\sin\left[\varphi - \varphi_n(r_*, c_1) + \frac{\pi}{2} \right]}\, dr_* =$$

$$= \frac{1}{\rho_* N_a} \frac{\Delta M_*}{\Delta R_1} \frac{1}{\pi D \sin\gamma}\, UEM(c_1, \varphi) \tag{23}$$

and the mean value:

$$\bar{U}_{eM}(c_1) = \frac{1}{\varphi_n(r_{*\max}, c_1) + \frac{\pi}{2}} \int_0^{\varphi_n(r_{*\max}, c_1) + \frac{\pi}{2}} U_{eM}(c_1, \varphi)\, d\varphi =$$

$$= \frac{1}{\varphi_n(r_{*\max}, c_1) + \frac{\pi}{2}} \frac{\frac{1}{\rho_* N_a} \frac{\Delta M_*}{\Delta R_1} \frac{1}{\pi D \sin\gamma}}{\int_0^\infty r_*^3 f_n(r_*, c_1)\, c_*(r_*, c_1)\, dr_*} \cdot \int_0^{\varphi_n(r_{*\max}, c_1) + \frac{\pi}{2}} \times$$

$$\times \int_0^\infty r_*^3 f_n(r_*, c_1)\, w_*(r_*, c_1) \left[\frac{w_{*N}(r_*, c_1, \varphi)}{2550} \right]^5 \times$$

$$\times \overline{\sin\left[\varphi - \varphi_n(r_*, c_1) + \frac{\pi}{2} \right]}\, dr_*\, d\varphi = \frac{1}{\rho_* N_a} \frac{\Delta M_*}{\Delta R_1} \frac{1}{\pi D \sin\gamma}\, \overline{UEM}(c_1) \,. \tag{24}$$

The following mean values of the impact velocity have been also introduced:

$$\underset{M}{\bar{w}}_{*N}(c_1, \varphi) = \int_0^\infty w_{*N}(r_*, c_1, \varphi) r_*^3 f_n(r_*, c_1)\, dr_* : \int_0^\infty r_*^3 f_n(r_*, c_1)\, dr_*, \tag{25}$$

$$\underset{M}{\bar{\bar{w}}}_{*N}(c_1) = \frac{1}{\left(\varphi_n + \frac{\pi}{2}\right) r_{*\max}} \int_0^{(\varphi_n+\frac{\pi}{2})(\varphi_n+\frac{\pi}{2}) r_{*\max}} \underset{M}{\bar{w}}_{*N}(c_1, \varphi)\, d\varphi. \tag{26}$$

The relevant programs of numerical calculations of these impact parameters are presented in ref. [6].

3. Some results of numerical calculation and it's relation to some experimental results

The theoretical analysis presented in the previous section and in ref. [6] had been triggered by interesting experimental results of B. Weigle and H. Severin [3]. They had found that for constant mass flux of water, G_W, supplied per unit width per unit time onto the plate, for constant circumferential velocity, u, of the sample but changing gas velocity c_1 in the range of

$$c_1 = 60\,\text{m/s} \text{ through } 75, 92, 153\,\text{m/s}$$

the erosion rate changes substantially. A fragment of the experimental results in the form of the relation $\Delta m = f(\tau)$ is shown in Fig. 5. The characteristic parameters $\Delta(\Delta m)/\Delta\tau$ and τ_0 for a sample of soft aluminum used in ref. [3] are tabulated below:

c_1 [m/s]	75	92	116	153	m/s
$\frac{\Delta(\Delta m)}{\Delta\tau}$	0.482	0.199	0.076	0.020	mg/min
τ_0	143	222	318	374	min

There are also shown the droplet size distribution functions relevant to the gas velocity c_1. It is apparent that with the increase of gas velocity c_1 the dispersion of the droplets increases, and the representative mean value of the droplet size

$$r_{*m}^3 = \int_0^\infty r_*^3 f_n(r_*, c_1)\, dr_* \tag{27}$$

decreases, as does the erosion rate represented by the ratio $\Delta(\Delta m)/\Delta\tau$ defined in Fig. 4. The complex of experimentaly established constants N_1, N_2 and N_3 introduced in eq. (4) is given below:

c_1 [m/s]	60	75	92	153
N_1	$2.096 \cdot 10^{23}$	$4.828 \cdot 10^{14}$	$5.077 \cdot 10^{34}$	$5.519 \cdot 10^{2}$
N_2	4.602	2.293	6.547	4.561
N_3	$3.039 \cdot 10^{4}$	$3.877 \cdot 10^{4}$	$1.090 \cdot 10^{5}$	$1.335 \cdot 10^{5}$

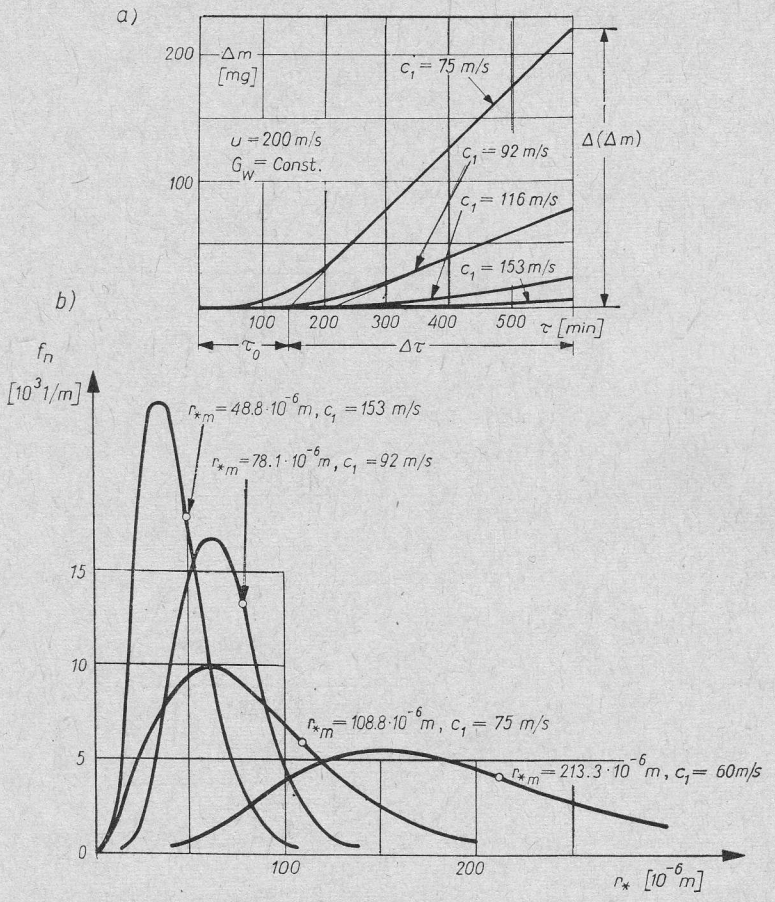

Fig. 5. Fragments of the experimental results of erosion damage-time patterns and droplet stream structure for the I.F.F.M. experimental stand (ref. [3]); a) material removal-time patterns soft aluminum, b) droplet stream structure

This significant change in erosion rate may result from several different effects. One of these may be the change in amount of water impacting the sample per unit area and unit time. As a matter of fact, Heymann's empirical relation (eq. (20)) says that the maximum instantaneous value of erosion rate $\Delta(\Delta m)/\Delta\tau \equiv U_{eM}$ is proportional to the volumetric water flux U_a over the eroded surface of the sample. The other reason for the change of experimental value of $\Delta(\Delta m)/\Delta\tau$ may be the change in the term $(w_{*N}/2550)^5$.

In order to shed more light on the problem the numerical calculations have been launched.

Numerical calculations presented in this section have been performed for the following set of parameters relevant to the stand of I.F.F.M.:

$$c_1 = 60, 75, 92, 153\ \mathrm{m/s}, \quad u = 200\ \mathrm{m/s}, \quad \gamma = 80°,$$

$$\Delta r_* = 10 \cdot 10^{-6}\ \mathrm{m}, \quad \mu = 1.85 \cdot 10^{-5}\ \mathrm{kg/ms},$$

$$\rho = 1.205\ \mathrm{kg/m^3}, \quad \rho_* = 1000\ \mathrm{kg/m^3}, \quad z = 0.3\ \mathrm{m}.$$

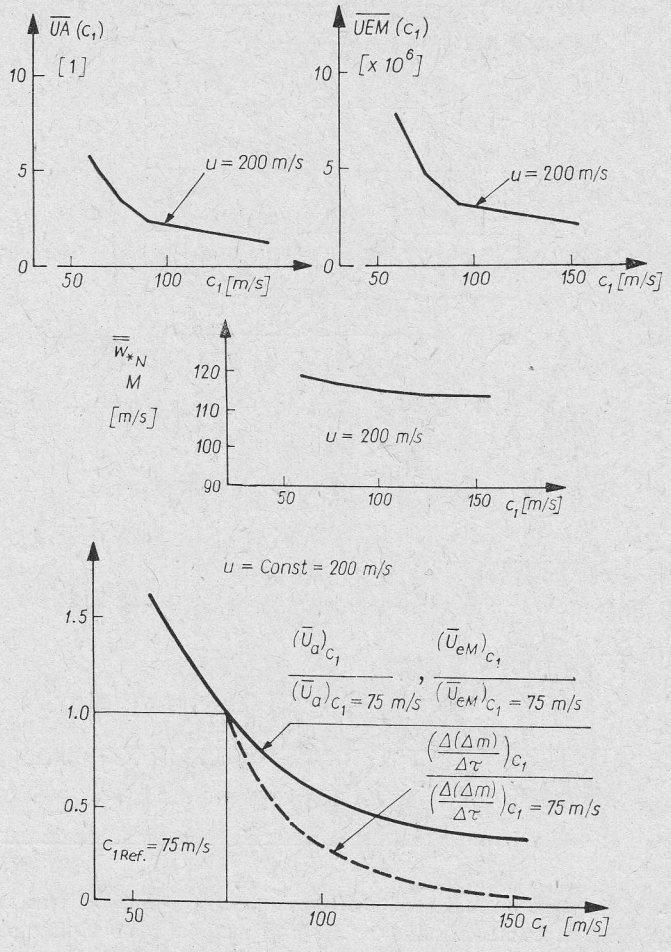

Fig. 6. Some of the theoretically calculated droplet impact parameters; $\overline{UA}(c_1)$, $\overline{UEM}(c_1)$, $\overline{\overline{w}}_{*N}(c_1)$, $(\bar{U}_a)_{c_1}/(\bar{U}_a)_{c_1=75\text{m/s}}$ and $(\bar{U}_{eM})_{c_1}/(\bar{U}_{eM})_{c_1=75\text{m/s}}$ calculated theoretically, $\left(\frac{\Delta(\Delta m)}{\Delta\tau}\right)_{c_1}\Big/\left(\frac{\Delta(\Delta m)}{\Delta\tau}\right)_{c_1=75}$ established experimentally

In Fig. 6 the results of numerical calculations of $\overline{UA}$ and $\overline{UEM}$ are presented. Both $\overline{UA}$ and $\overline{UEM}$ are proportional to $\bar{U}_a$ and $\bar{U}_{eM}$ respectively (see eq. (19), (24)). $\bar{U}_a$ and $\bar{U}_{eM}$ decrease, as does the experimental value $\Delta(\Delta m)\,\Delta\tau$ when c_1 increases. The trend of change of both theoretical and experimental values is the same. However, it may be readily shown that

$$\left(\frac{\Delta(\Delta m)}{\Delta\tau}\right)_{c_1}\Big/\left(\frac{\Delta(\Delta m)}{\Delta\tau}\right)_{c_1=75\text{m/s}}$$

changes much faster than do $\overline{UA}_{c_1}/\overline{UA}_{c_1=75}$ and $\overline{UEM}_{c_1}/\overline{UEM}_{c_1=75}$. For $c_1=153$ m/s there is already a difference in order of magnitude between the theoretical and experimental

values. This difference clearly may not be explained as the consequence of averaging, or the assumption concerning the superposition of erosion caused by the droplet groups of particular size.

In searching for a reason for this discrepancy, attention must be paid to the problem of the correlation between the droplet stream structure and the erosion rate pattern. The program of experiments of B. Weigle and H. Severin is particularly suitable for these investigations because their stand makes it possible to change the droplet stream structure easily for almost unchanged mean impact velocity $\overline{w}_{*N}$ (Fig. 6).

Little is known, however, about the droplet size–erosion rate relationship, and only in exceptional experiments was the droplet size investigated. However, it has been indicated (ref. [2]) that the droplet size is probably related to the maximum instantaneous value of rationalized erosion rate, through the influence on its threshold value. The rationalized erosion rate has been defined in ref. [2] as follows:

$$E_r = \frac{\text{Volume of material lost per unit area per unit time}}{\text{Volume of liquid impinged per unit area per unit time}}.$$

In the nomenclature of this report:

– Volume of material lost per unit area per unit time =

$$= \Delta(\Delta m)\frac{1}{\rho_s}/\Delta\tau \cdot L_s \cdot \pi \cdot \frac{D_s}{2}$$

and

– Volume of liquid impinged per unit area per unit time =

$$= \bar{U}_a = \frac{1}{\rho_* N_a}\frac{\Delta M_*}{\Delta R_1}\frac{1}{\pi D \sin\gamma}\overline{UA}.$$

Hence

$$E_r(c_1) \sim \frac{\Delta(\Delta m)/\Delta\tau}{\overline{UA}}.$$

As indicated above $\Delta(\Delta m)/\Delta\tau$ has been established experimentally, $\overline{UA}$ is calculated in this report, so that $E_r(c_1)$ related to I.F.F.M. experiments may be readily found.

In ref. [2] Heymann suggests the droplet size–erosion rate dependence in the form of the following possible relations:

$$E_r = f_1\left[w_{*N}\left(1-\frac{G}{w_{*N}^2 r_*}\right)\right] \quad \text{or} \quad E_r = f_2\left[w_{*N}-\sqrt{\frac{G}{r_*}}\right]. \tag{28}$$

For both of these relations which, strictly speaking, are not yet fully confirmed by experiment, the terms $G/(w_{*N}^2 r_*)$ and $\sqrt{G/r_*}$ relate to the threshold impact velocity w_{*Nc} such that for $w_{*N} \leqslant w_{*Nc}$ no erosion results. G may be considered as a material constant. Now, the experimental data of (ref. [3]) for an aluminum sample, partially quoted in Fig. 5, may be used to determine this constant G, and thus the relationship between w_{*Nc} and r_*. It may be done by means of the plot $E_r = f(r_*)$ (see Fig. 7a) because in the experiments mentioned the mean value of the impact velocity w_{*N} was almost constant. In fact, for

$u=200$ m/s the mean impact velocity changes only between

$$\bar{\bar{w}}_{*N}=119\,;\ 117.1\,;\ 115.5 \text{ and } 113.5\,\text{m/s}$$

for

$$c_1=60\,;\ 75\,;\ 92 \text{ and } 153\,\text{m/s respectively}$$

(see Fig. 6).

Thus, from the appropriate extrapolation of the function $E_r=f(r_*)$ (see Fig. 7a), for a given impact velocity $\bar{\bar{w}}_{*N}=\sim 116$ m/s, results the threshold droplet size $r_{*c}=44\cdot 10^{-6}$ m. Hence, for the material considered*

$$G=d_{*c}\,\bar{\bar{w}}^2_{*N}=1{,}185\,\text{m}^3/\text{s}^2\,.$$

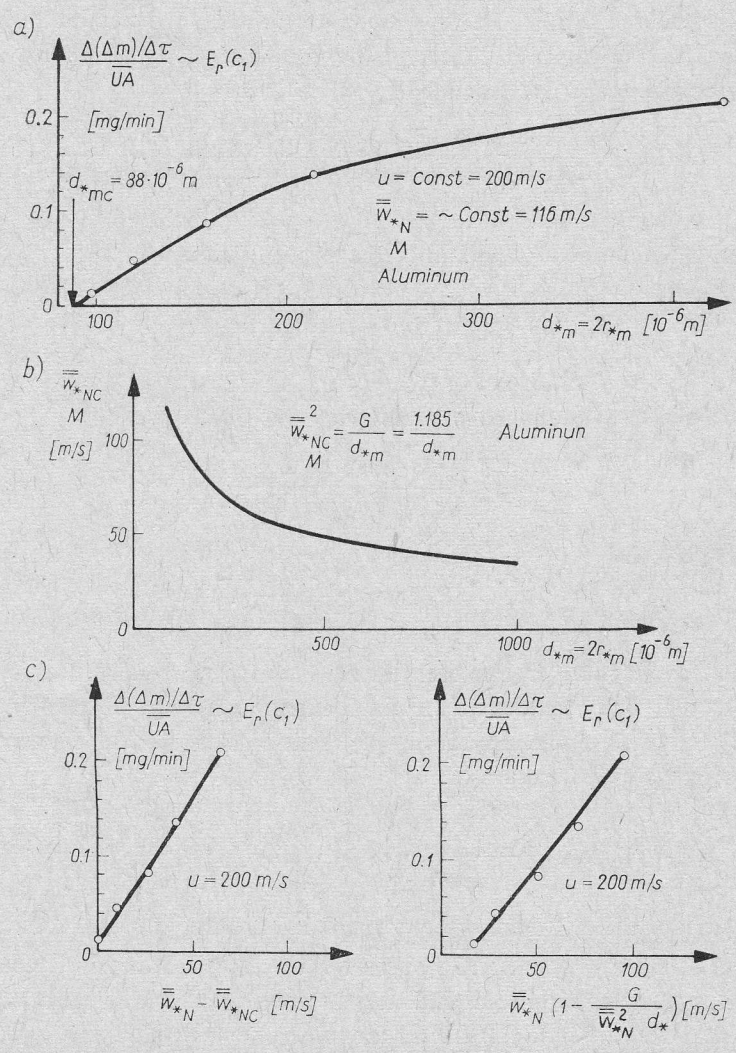

Fig. 7. Threshold combination of velocity and droplet size (soft aluminum, see foot note on page 93); $\Delta(\Delta m)/\Delta\tau$ obtained from the experiment, $\overline{UA}$ calculated acc. to the eq. (19)

The results of the Busch and Hoff experiments (ref. [2]) may be here recollected. They obtained for the rain-eroded aluminum the threshold velocity $w_{*Nc} = \sim 33$ m/s. Hence the corresponding droplet size d_* would be of order $1 \cdot 10^{-3}$ m which appears qualitatively reasonable for the rain droplet size.

Fig. 7c shows that when E_r is plotted versus $\bar{\bar{w}}_{*N} - \bar{\bar{w}}_{*Nc}$ better correlation results than in the case of the plott E_r versus $\bar{\bar{w}}_{*N}\left(1 - \frac{G}{w_{*N}^2 d_*}\right)$.

It has to be pointed out here that in this report only a small part of the results of ref. [3] has been used. In addition, in assessment of r_{*c} and G, the results for only one velocity w_{*N} have been used. More extensive experimental data are needed to shed more light on the problem.

4. Conclusions

1. The experimental investigation of B. Weigle and H. Severin, published in ref. [3], indicated substantial dependence of the erosion damage-time patterns upon the droplet size.

2. These experimental results of I.F.F.M. deserve certainly some more consideration. To make it possible, a theoretical model of droplet impact for the experimental stand of I.F.F.M. has been presented in this report. Attention has been particularly paid to the calculations of the mean value of the volumetric water flux U_a over the sample surface. Also the mean value of the product of water flux, U_a, and $(W_{*N}/2550)^5$ as well as the mean impact velocity w_{*N} have been calculated.

3. Comparison of experimental and theoretical data indicated that the experimentally established rationalized erosion rate E_r changes faster with the gas velocity c_1 than theoretically calculated water flux U_a and the mean value U_{eM} of the product $U_a(w_{*N}/2550)^5$.

4. It is likely that variation in droplet size causes this discrepancy. The threshold droplet size of order $r_* = \sim 44 \cdot 10^6$ m for mean impact velocity $w_{*N} = \sim 116$ m/s for soft aluminum has been established under the assumption (ref. [2]) that the droplet size effect can be represented by a factor of the form:

$$w_{*N}^2 r_* = \text{const} = G .$$

5. The model presented of the droplet impact indicated that the experimental stand of I.F.F.M. is particularly suitable for experiments designed to shed more light on the problem of droplet size effect:

– it provides the possibility of the exceptional change of the mean droplet size between $r_* = \sim 50 \cdot 10^{-6}$ m up to about $r_* = \sim 300 \cdot 10^{-6}$ m,

– the mean value of the impact velocity may be controlled independently,

– the droplet stream structure seems to approach the stream structure in the steam turbine.

---

* Aluminum PA6 (Polish Standards PN-59/H-88026: 3,8÷4,8% Cu, 0,4÷0,8% Mg, 0,4÷÷0,8% Mn, $R_c \cong 38$ kG/mm², $Rm \cong 48{,}5$ kG/mm², $a_5 \cong 12\%$, $HB \cong 130$).

6. Further investigation of the relationship between the erosion resistance and the droplet size are of importance because in ref. [1] it has been already shown that the impact parameters are also seriously influenced by the droplet stream structure. Thus the control of the droplet stream structure may offer a powerful method for the protection of steam turbine blading.

Acknowledgments. This report has been prepared during the author's sabbatical year in the United States, which was arranged in the exchange program between the Polish Academy of Sciences, Warsaw, and the National Academy of Sciences, Washington, D. C. The author appreciates the assistance of his hosts in the United States: Professor J. R. Moszynski of the University of Delaware and Professor F. G. Hammitt of the University of Michigan. The author is also indebted to his colleagues Mr. B. Weigle and Mr. H. Severin for supplying some of their experimental results before publication (ref. [3]). Finally, the author is grateful to Mr. Frank J. Heymann for numerous discussions which stimulated preparation of this report.

Received by the Editor, February 1974.

References

[1] J. Krzyżanowski, *The Correlation Between Droplet Stream Structure and Steam Turbine Blading Erosion.* Transaction ASME, Paper No. 73-Pwr-B. 1973, Journal of Engineering for Power, V. 63, No. 3, July, 1974.

[2] W. D. Pouchot, F. J. Heymann, *et al.*, *Basic Investigation of Turbine Erosion Phenomena.* NASA Contractor Report, NASA C 1830, November, 1971.

[3] B. Weigle, H. Severin, *The Investigation of the Relationship Between the Gas Velocity, theDroplet Stream Structure and the Erosion Rate-Time Pattern* (in Polish). Report of IFFM, No. 273/71 Gdańsk, Poland, December, 1971.

[4] F. J. Heymann, *Toward Quantitative Prediction of Liquid Impact Erosion.* ASTM STP 474, American Society of Testing and Materials, pp. 212 - 248, 1970.

[5] J. Krzyżanowski, *On the Problems of Liquid Phase Motion in a Steam Turbine Stage* (in Polish). PWN, Warszawa – Poznań 1969.

[6] J. Krzyżanowski, *On the Erosion Rate – Droplet Size Relation for an Experimental Stand with a Rotating Sample.* Report No UMICH 03371-17-T, Department of Mechanical Engineering, University of Michigan, May, 1972.

O relacji między wielkością kropel i szybkością erozji

Streszczenie

Dotychczas stosunkowo mało wiadomo o związku między wielkością kropel, a szybkością erozji łopatek turbin parowych. Wskazano wprawdzie na drodze teoretycznej, że struktura strumienia kropel może w istotny sposób wpływać na niektóre parametry kolizji kropel z łopatką turbinową [1]. By rzucić jednakże więcej światła na to zagadnienie, uruchomiono w Instytucie Maszyn Przepływowych PAN serię badań eksperymentalnych na stoisku umożliwiającym łatwą zmianę struktury strumienia kropel. Celem tego opracowania jest zaprezentowanie algorytmu wiążącego strukturę strumienia kropel we wspomnianym stoisku z niektórymi parametrami kolizji. Uczyniono również próbę wstępnej analizy niektórych wyników doświadczeń [3].

Зависимость между величиной капель и скоростью зрозионного процесса

Резюме

До сих пор относительно немного известно о зависимости между величиной капель и скоростью процесса эрозии лопаток паровых турбин. По правде, указывается на основе теоретических рассуждений на факт, что структура потока капель может в самом деле влиять на некоторые параметры коллизии капель с турбинной лопаткой [1]. Для лучшего выяснения этого вопроса в Институте проточных машин ПАН проведена серия экспериментальных исследований эрозии на стенде, позволяющем легко менять структуру потока капель. Целью этой работы является определение алгоритма, связывающего структуру потока капель на указанном стенде с некоторыми параметрами коллизии. Сделана также попытка проведения вступительного анализа некоторых результатов исследований [3].